

# Theoretical Study of Polarization Observables For The $\gamma d \rightarrow \pi NN$ Reaction in the $\Delta(1232)$ -Resonance Region

E. M. Darwish<sup>1,2,\*</sup>, H. M. Abou-Elsebaa<sup>1,2</sup>, and A. E. Elmeshneb<sup>1,3</sup>

<sup>1</sup>Physics Department, Faculty of Science, Sohag University, Sohag 82524, Egypt

<sup>2</sup>Physics Department, College of Science, Taibah University, Medina 41411, Saudi Arabia

<sup>3</sup>Physics Department, College of Science and Arts, Taibah University, Al-Ula Branch, Saudi Arabia

Received: 12 May 2021, Revised: 7 Aug. 2021, Accepted: 25 Aug. 2021

Published online: 1 Sep. 2021

**Abstract:** Incoherent pion photoproduction on the deuteron in the  $\Delta(1232)$ -resonance region is investigated with special emphasis on polarization observables. For the elementary pion photoproduction operator an effective Lagrangian model which includes the standard pseudovector Born terms and a resonance contribution from the  $\Delta(1232)$ -excitation is used. Our results for the elementary  $\gamma N \rightarrow \pi N$  reaction are in good agreement with recent experimental data and results of other theoretical calculations. A general analysis of all possible polarization observables for the  $\gamma d \rightarrow \pi NN$  reaction with polarized photon beam and/or oriented deuteron target is presented. The unpolarized differential cross section, photon asymmetry, vector and tensor target asymmetries are predicted for forthcoming experiments.

**Keywords:** Polarization phenomena in reactions, Meson production, Photoproduction reactions, Few-body systems

## 1 Introduction

During the last two decades, pseudoscalar meson production in electromagnetic reactions on light nuclei has become a very active field of research in medium-energy nuclear physics with respect to the study of hadron structure [1, 2, 3, 4, 5, 6, 7, 8, 9, 10, 11, 12, 13, 14, 15, 16, 17, 18, 19, 20, 21, 22]. For the following reasons the deuteron plays an outstanding role besides the free nucleon. The first one is that the deuteron is the simplest nucleus on whose structure we have abundant information and a reliable theoretical understanding, i.e., the structure of the deuteron is very well understood in comparison to heavier nuclei. Furthermore, the small binding energy of nucleons in the deuteron, which from the kinematical point of view provides the case of a nearly free neutron target, allows one to compare the contributions of its constituents to the electromagnetic and hadronic reactions to those from free nucleons in order to estimate interaction effects.

Meson photo- and electroproduction on light nuclei is primarily motivated by the following possibilities: (i) study of the elementary neutron amplitude in the absence of a neutron target, (ii) investigation of medium effects,

i.e., possible changes of the production operator in the presence of other nucleons, (iii) it provides an interesting means to study nuclear structure, and (iv) it gives information on pion production on off-shell nucleon, as well as on the very important  $\Delta N$ -interaction in a nuclear medium. As an illustration of these various aspects, we will investigate in this paper incoherent pion photoproduction on the deuteron in the  $\Delta(1232)$ -resonance region with special emphasis on polarization observables. The importance of this process derives from the fact that the deuteron, being the simplest nuclear system, plays a similar fundamental role in nuclear physics as the hydrogen atom plays in atomic physics.

The major reason for studying polarization phenomena in reactions of the type  $a + b \rightarrow c + d + \dots$  lies in the fact that only the use of polarization degrees of freedom allows one to obtain complete information on all possible reaction matrix elements. Without polarization, the cross section is given by the incoherent sum of squares of the reaction matrix elements only. Thus, small amplitudes are masked by the dominant ones. On the other hand, small amplitudes very often contain interesting information on subtle dynamical effects. This

\* Corresponding author e-mail: [darwish@science.sohag.edu.eg](mailto:darwish@science.sohag.edu.eg)

is the place where polarization observables enter, because such observables in general contain interference terms of the various matrix elements in different ways. Thus, a small amplitude may be considerably amplified by the interference with a dominant matrix element. An example is provided by the influence of the small electric form factor of the neutron on the transverse in-plane component of the neutron polarization in quasifree deuteron electrodisintegration [23,24,25]. It is just this feature for which polarization physics has become such an important topic in various branches of physics.

The present paper is a natural extension of our work in [26,27] where we have presented the energy dependence of the  $\gamma d \rightarrow \pi NN$  reaction over the whole  $\Delta(1232)$ -resonance region and gave results for differential and total cross sections as well as results for the spin asymmetry and Gerasimov-Drell-Hearn (GDH) sum rule for the deuteron. Notwithstanding this continuing effort to study this process, the wealth of information contained in it has not yet been fully exploited. Since the  $t$ -matrix has 12 independent complex amplitudes, one has to measure 23 independent observables, in principle, in order to determine completely the  $t$ -matrix. Up to present times, only a few observables have been measured and studied in detail, e.g., differential and total cross sections.

On the other hand, the measurement of polarization observables is a rather difficult task, requiring great experimental skill and advanced technology, which explains why little is known about these more involved polarization observables. However, in view of the recent technical improvements, e.g., at MAMI in Mainz, ELSA in Bonn and JLab in Newport News, for preparing polarized beams and targets and for polarimeters for the polarization analysis of ejected particles it appears timely to study in detail polarization observables in pion production on the deuteron. The aim will be to see what kind of information is buried in the various polarization observables, in particular, what can be learned about the role of subnuclear degrees of freedom like meson and isobar or even quark-gluon degrees of freedom.

The paper is organized as follows. In Section 2 we will present the effective Lagrangian model for the elementary pion photoproduction amplitude which will serve as an input for the reaction on the deuteron. Its predictions for differential and total cross sections are compared with recent experimental data and results of other theoretical predictions. Section 3 will introduce the general form of the differential cross section for incoherent pion photoproduction on the deuteron. The treatment of the  $\gamma d \rightarrow \pi NN$  amplitude, based on time-ordered perturbation theory, will be described in Section 4. In Section 5 we will give the complete formal expressions of polarization observables for the  $\gamma d \rightarrow \pi NN$  reaction with polarized photon beam and/or oriented deuteron target in terms of the  $t$ -matrix elements. Details of the actual calculation and the results will be presented and discussed in Section 6. Finally, we close in Section 7 with conclusions.

## 2 The $\gamma N \rightarrow \pi N$ amplitude

For the elementary pion photoproduction operator, we have taken, as in our previous work [26,27], the effective Lagrangian model of Schmidt *et al.* [28]. This model had been constructed to give a realistic description of the  $\Delta(1232)$ -resonance region. It is given in an arbitrary frame of reference and allows a well defined off-shell continuation as required for studying pion production on nuclei. It is in contrast to other approaches, where the elementary amplitude is constructed first on-shell in the photon-nucleon center-of-mass (c.m.) frame with subsequent boost into an arbitrary reference frame and some prescription for the off-shell continuation. In the latter method, one loses terms which by chance vanish in the c.m. frame [29]. In our approach, the only uncertainty arises from the assignment of the invariant energy for the photon-nucleon subsystem in the resonance propagators as has been discussed in detail in [29]. Here we use the spectator on-shell approach. The model of Schmidt *et al.* [28] consists of the standard pseudovector Born terms and the contribution of the  $\Delta(1232)$ -resonance. The individual terms of the matrix element for pion photoproduction reaction on the free nucleon are shown in Fig. 1. For further details with respect to the elementary pion photoproduction operator we refer to [28]. The parameters of the  $\Delta$ -resonance are fixed by fitting the experimental  $M_{1+}^{3/2}$  multipole which is dominant in the region of the  $\Delta$ -resonance. The quality of the model can be judged by a comparison with the MAID analysis [30], the Mainz dispersion analysis [31], and the VPI analysis [32] as shown in Fig. 2, and one notes quite a good agreement.

In Fig. 3 we compare our results for the differential cross sections with the MAID analysis [30] and with experimental data. For  $\pi^+$  and  $\pi^0$  photoproduction on the proton the data are taken from [33] (TAPS), [34] (MAMI) and [35] (GDH), whereas for  $\pi^-$  photoproduction on the neutron we took the data of the inverse reaction  $\gamma n \leftarrow p\pi^-$  from [36] (Tokyo). In general, we obtain quite a good agreement with the data, especially in the region of the  $\Delta(1232)$ -resonance (330 MeV). Also in comparison with the MAID analysis our elementary production operator does quite well in this energy region. One notes only small discrepancies which very likely come from the fact that no other resonances besides the  $\Delta(1232)$  are included in our model.

The total cross sections for the different pion channels are shown in Fig. 4 and compared with experimental data. In general, we obtain a good agreement with the data using the small value  $f_{\pi N}^2/4\pi = 0.069$  for the pion-nucleon coupling constant. The agreement with the data from [36] and [37] for  $\pi^-$  photoproduction is again satisfactory. In case of the  $\pi^+$  photoproduction, the agreement is good up to a photon energy of about 400 MeV. For higher energies, the  $D_{13}$ -resonance, which is not included in our calculation, gives a non-vanishing contribution [30]. The  $\pi^+$  data from [36] are slightly

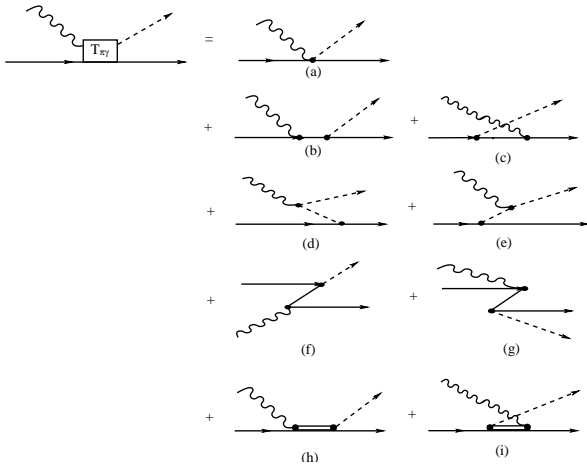


**Fig. 1:** Diagrams for the elementary process  $\gamma N \rightarrow \pi N$ : (a) the Kroll-Rudermann graph, (b) and (c) the two time-ordered contributions to the direct and crossed nucleon pole graph, (d) and (e) the two time-ordered contributions to the pion pole graph, (f) and (g) the Z-graphs, and (h) and (i) the  $\Delta(1232)$ -resonance graphs. A solid, dashed and wavy lines represent a nucleon, pion and photon, respectively.

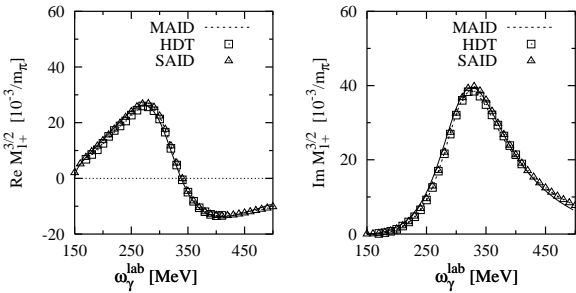


**Fig. 2:** Real and imaginary parts of the  $M_{1+}^{3/2}$  multipole. Notation: solid curves: present model; dotted curves: MAID [30]. Data points: from [32] (SAID, solution: September 2000), [31] (HDT).

underestimated in the resonance region by our calculation but also by the MAID analysis. Except for a tiny overestimation in the maximum, the description of the data from [35,38] for  $\pi^0$  production on the proton is also very good. Therefore, this model for the elementary photoproduction amplitude is quite satisfactory for our purpose, namely to incorporate it into the reaction on the deuteron.

### 3 Process on the deuteron

In this section we will briefly review the general formalism for incoherent pion photoproduction on the deuteron. The general expression for the 5-fold unpolarized differential cross section of pion

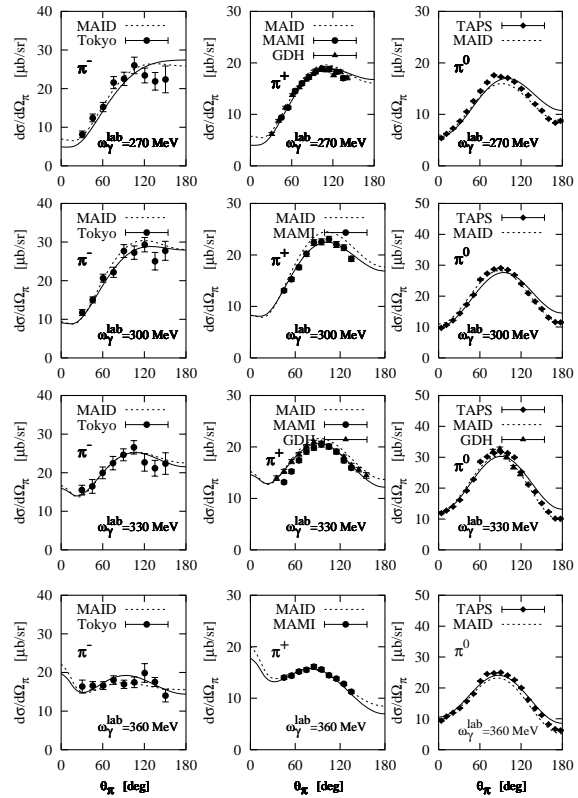


**Fig. 3:** Differential cross section for the elementary reaction on the nucleon for the three charge states of the pion at various photon energies. Left panels:  $\pi^{-}$ , middle panels:  $\pi^{+}$ , and right panels:  $\pi^0$ . The solid curves: present model; dotted curves: MAID [30]. Experimental data from [36] (Tokyo) for  $\pi^{-}$ , [34] (MAMI), [35] (GDH) for  $\pi^0$ , and [33] (TAPS), [35] (GDH) for  $\pi^{+}$ .

photoproduction reaction on the deuteron is given, using the conventions of Bjorken and Drell [39], by

$$d\sigma = (2\pi)^{-5} \delta^4(k + d - p_1 - p_2 - q) \frac{1}{|\mathbf{v}_{\gamma} - \mathbf{v}_d|} \times \frac{1}{2} \frac{d^3 q}{2\omega_{\mathbf{q}}} \frac{d^3 p_1}{E_1} \frac{d^3 p_2}{E_2} \frac{M_N^2}{4\omega_{\gamma} E_d} \frac{1}{6} \sum_{\alpha} |\mathcal{M}_{sm\gamma m_d}^{(t\mu)}|^2, \quad (1)$$

where we have introduced as a shorthand for the quantum numbers  $\alpha = (s, m, t, m_{\gamma}, m_d)$ . The initial photon and deuteron four-momenta are denoted by  $k = (\omega_{\gamma}, \mathbf{k})$  and  $d = (E_d, \mathbf{d})$ , respectively, and the four-momenta of final meson and two nucleons by  $q = (\omega_q, \mathbf{q})$  with  $\omega_q = \sqrt{m_{\pi}^2 + \mathbf{q}^2}$ ,  $m_{\pi}$  as pion mass, and  $p_j = (E_j, \mathbf{p}_j)$  ( $j = 1, 2$ ) with  $E_j = \sqrt{M_N^2 + \mathbf{p}_j^2}$ , respectively, and  $M_N$  as nucleon mass. Furthermore,  $m_{\gamma}$  denotes the photon polarization,  $m_d$  the spin projection of the deuteron,  $s$  and  $m$  total spin and projection of the two outgoing nucleons, respectively,  $t$  their total isospin,  $\mu$  the isospin projection of the pion, and  $\mathbf{v}_{\gamma}$  and  $\mathbf{v}_d$  the velocities of photon and deuteron, respectively. The states of all particles are

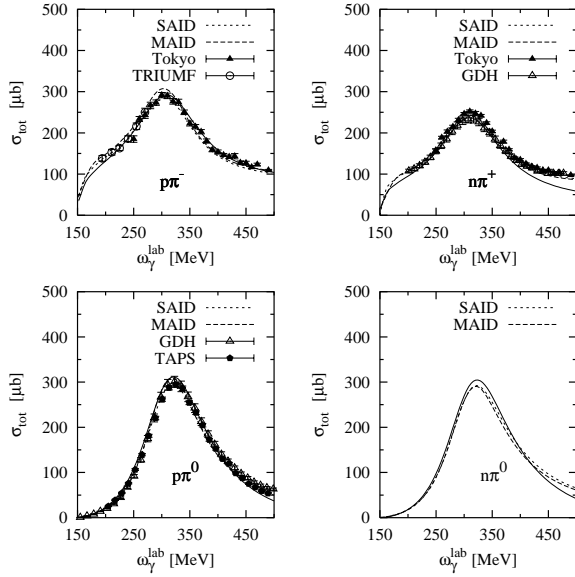


**Fig. 4:** Total cross sections for pion photoproduction on the nucleon as a function of photon energy for all four physical channels. Notation of the curves: solid: present model; dotted: SAID [32]; dashed: MAID [30]. Experimental data from [36] (Tokyo), [37] (TRIUMF), [35] (GDH), [38] (TAPS).

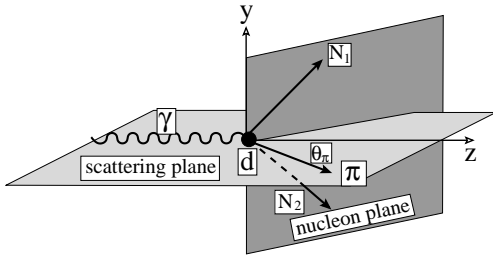


**Fig. 5:** Kinematics in the laboratory system for  $\gamma d \rightarrow \pi NN$ .

covariantly normalized. The reaction amplitude is denoted by  $\mathcal{M}_{s\text{mm}\gamma m_d}^{(t\mu)}$ . As in [26,27,28], we have chosen as independent variables the pion momentum  $q$ , its angles  $\theta_\pi$  and  $\phi_\pi$ , the polar angle  $\theta_{P_{NN}}$  and the azimuthal angle  $\phi_{P_{NN}}$  of the relative momentum  $\mathbf{p}_{NN}$  of the two outgoing nucleons as independent variables. We prefer this choice of variables, because in this case the kinematic factor do not has any singularity on the boundary of the available phase space, when  $p_{NN} \rightarrow 0$ .

The total and relative momenta of the final  $NN$ -system are defined respectively by

$$\mathbf{P}_{NN} = \mathbf{p}_1 + \mathbf{p}_2 = \mathbf{k} - \mathbf{q} \quad (2)$$

and

$$\mathbf{p}_{NN} = \frac{1}{2}(\mathbf{p}_1 - \mathbf{p}_2). \quad (3)$$

The absolute value of the relative momentum  $\mathbf{p}_{NN}$  is given by

$$p_{NN} = \frac{1}{2} \sqrt{\frac{E_{NN}^2 (W_{NN}^2 - 4M_N^2)}{E_{NN}^2 - P_{NN}^2 \cos^2 \theta_{P_{NN}}}}, \quad (4)$$

where  $\theta_{P_{NN}}$  is the angle between  $\mathbf{P}_{NN}$  and  $\mathbf{p}_{NN}$ .  $E_{NN}$  and  $W_{NN}$  denote total energy and invariant mass of the  $NN$ -subsystem, respectively, and are given by

$$E_{NN} = E_1 + E_2 = \omega_\gamma + E_d - \omega_q, \\ W_{NN}^2 = E_{NN}^2 - P_{NN}^2. \quad (5)$$

For the evaluation we have chosen the laboratory frame where  $d^\mu = (M_d, \mathbf{0})$  with  $M_d$  as deuteron mass. As coordinate system a right-handed one is taken with  $z$ -axis along the momentum  $\mathbf{k}$  of the incoming photon and  $y$ -axis along  $\mathbf{k} \times \mathbf{q}$ . Thus, the outgoing pion defines the scattering plane. Another plane is defined by the momenta of the outgoing nucleons which we will call the nucleon plane (see Fig. 5).

The fully exclusive differential cross section is given by

$$\frac{d^5\sigma}{d\Omega_{P_{NN}} d\Omega_\pi dq} = \frac{\rho_s}{6} \sum_{\alpha} |\mathcal{M}_{s\text{mm}\gamma m_d}^{(t\mu)}|^2, \quad (6)$$

where the phase space factor  $\rho_s$  is expressed in terms of relative and total momenta of the two final nucleons

$$\rho_s = \frac{1}{(2\pi)^5} \frac{q^2}{16\omega_\gamma M_d \omega_q} \\ \times \frac{p_{NN}^2 M_N^2}{|E_2(p_{NN} + \frac{1}{2}P_{NN} \cos \theta_{P_{NN}}) + E_1(p_{NN} - \frac{1}{2}P_{NN} \cos \theta_{P_{NN}})|}. \quad (7)$$

## 4 The $\gamma d \rightarrow \pi NN$ amplitude

A plane wave impulse approximation usually serves as the starting point to calculate the amplitude for electromagnetic pion production on the deuteron [40,41,42,43] or on a nucleus in general. It corresponds to a direct embedding of the elementary amplitudes into the two-nucleon system. The general form of the photoproduction transition matrix is given by

$$\mathcal{M}_{s\text{mm}\gamma m_d}^{(t\mu)}(\mathbf{k}, \mathbf{q}, \mathbf{p}_1, \mathbf{p}_2) = \langle \mathbf{q}, \mu, \mathbf{p}_1, \mathbf{p}_2 | s m t - \mu | \varepsilon_\mu(m_\gamma) \\ \times J^\mu(0) | \mathbf{d} m_d 00 \rangle, \quad (8)$$

where  $J^\mu(0)$  denotes the current operator and  $\varepsilon_\mu(m_\gamma)$  the photon polarization vector. The electromagnetic interaction consists of the elementary production process on one of the nucleons  $T_{\pi\gamma}^{(j)}$  ( $j = 1, 2$ ) and in principle a possible irreducible two-body production operator  $T_{\pi\gamma}^{(NN)}$ . The final  $\pi NN$  state is then subject to the various hadronic two-body interactions as described by an half-off-shell three-body scattering amplitude  $T^{\pi NN}$ . In the following, we will neglect the electromagnetic

two-body production  $T_{\pi\gamma}^{(NN)}$  and the outgoing  $\pi NN$  scattering state is approximated by the free  $\pi NN$  plane wave, i.e.,

$$|\mathbf{q}\mu, \mathbf{p}_1\mathbf{p}_2 smt - \mu\rangle^{(-)} = |\mathbf{q}\mu, \mathbf{p}_1\mathbf{p}_2 smt - \mu\rangle. \quad (9)$$

This means, we include only the pure plane wave impulse approximation (IA), which is defined by the electromagnetic pion production on one of the nucleons alone, while a more realistic treatment including final state interaction as well as two-body effects will be reported in a forthcoming paper. Our justification for such a procedure is the fact that the IA is the primary process which will be gauged against all other effects.

For the spin ( $|sm\rangle$ ) and isospin ( $|t - \mu\rangle$ ) part of the two nucleon wave functions we use a coupled spin-isospin basis  $|sm, t - \mu\rangle$ . The antisymmetric final  $NN$  plane wave function thus has the form

$$|\mathbf{p}_1, \mathbf{p}_2, sm, t - \mu\rangle = \frac{1}{\sqrt{2}} \left( |\mathbf{p}_1\rangle^{(1)} |\mathbf{p}_2\rangle^{(2)} - (-)^{s+t} |\mathbf{p}_2\rangle^{(1)} |\mathbf{p}_1\rangle^{(2)} \right) \times |sm, t - \mu\rangle, \quad (10)$$

where the superscript indicates to which particle the ket refers. In the case of charged pions, only the  $t = 1$  channel contributes whereas for  $\pi^0$  production both  $t = 0$  and  $t = 1$  channels have to be taken into account. Then, the matrix element is given by

$$\begin{aligned} \mathcal{M}_{smm_\gamma m_d}^{(t\mu)}(\mathbf{k}, \mathbf{q}, \mathbf{p}_1, \mathbf{p}_2) &= \langle \mathbf{p}_1, \mathbf{p}_2, sm, t - \mu | t_{\gamma\pi}^{NN}(\mathbf{k}, \mathbf{q}) | \mathbf{d}m_d, 00 \rangle \\ &= \frac{1}{2} \int \frac{d^3 p'_1}{(2\pi)^3} \int \frac{d^3 p'_2}{(2\pi)^3} \frac{M_N^2}{E'_1 E'_2} \\ &\times \sum_{m'} \langle \mathbf{p}_1 \mathbf{p}_2, sm, t - \mu | t_{\gamma\pi}^{NN}(\mathbf{k}, \mathbf{q}) | \mathbf{p}'_1 \mathbf{p}'_2, 1m', 00 \rangle \\ &\times \langle \mathbf{p}'_1 \mathbf{p}'_2, 1m', 00 | \mathbf{d}m_d, 00 \rangle \end{aligned} \quad (11)$$

with

$$t_{\gamma\pi}^{NN}(\mathbf{k}, \mathbf{q}) = t_{\gamma\pi}^{N(1)}(\mathbf{k}, \mathbf{q}) + t_{\gamma\pi}^{N(2)}(\mathbf{k}, \mathbf{q}), \quad (12)$$

where  $t_{\gamma\pi}^{N(j)}$  denotes the elementary production amplitude on nucleon “ $j$ ”. As mentioned above, we use covariant normalization for the nucleon, deuteron and meson states, i.e.,

$$\begin{aligned} \langle \mathbf{p}' | \mathbf{p} \rangle &= (2\pi)^3 \frac{E_p}{M_N} \delta^3(\mathbf{p}' - \mathbf{p}), \\ \langle \mathbf{d}' | \mathbf{d} \rangle &= (2\pi)^3 2E_d \delta^3(\mathbf{d}' - \mathbf{d}), \\ \langle \mathbf{q}' | \mathbf{q} \rangle &= (2\pi)^3 2\omega_q \delta^3(\mathbf{q}' - \mathbf{q}). \end{aligned} \quad (13)$$

The deuteron wave function has the form

$$\begin{aligned} \langle \mathbf{p}_1 \mathbf{p}_2, 1m, 00 | \mathbf{d}m_d, 00 \rangle &= (2\pi)^3 \delta^3(\mathbf{d} - \mathbf{p}_1 - \mathbf{p}_2) \\ &\times \frac{\sqrt{2E_1 E_2}}{M_N} \tilde{\Psi}_{m, m_d}(\mathbf{p}_{NN}) \end{aligned} \quad (14)$$

with

$$\tilde{\Psi}_{m, m_d}(\mathbf{p}) = (2\pi)^{\frac{3}{2}} \sqrt{2E_d} \sum_{L=0,2} \sum_{m_L} i^L C_{m_1 m_2 m}^{j_1 j_2 j} u_L(p) Y_{L m_L}(\hat{p}), \quad (15)$$

denoting with  $C_{m_1 m_2 m}^{j_1 j_2 j}$  a Clebsch-Gordan coefficient,  $u_L(p)$  the radial deuteron wave function and  $Y_{L m_L}(\hat{p})$  a spherical harmonics. Using (12) one finds in the laboratory system for the matrix element the following expression

$$\begin{aligned} \mathcal{M}_{smm_\gamma m_d}^{(t\mu)}(\mathbf{k}, \mathbf{q}, \mathbf{p}_1, \mathbf{p}_2) &= \sqrt{2} \sum_{m'} \langle sm, t - \mu | \\ &\times \left( \langle \mathbf{p}_1 | t_{\gamma\pi}^{N(1)}(\mathbf{k}, \mathbf{q}) | - \mathbf{p}_2 \rangle \tilde{\Psi}_{m', m_d}(\mathbf{p}_2) \right. \\ &\left. - (-)^{s+t} \langle \mathbf{p}_1 \leftrightarrow \mathbf{p}_2 \rangle \right) | 1m', 00 \rangle. \end{aligned} \quad (16)$$

Note, that in (16) the elementary production operator acts on nucleon “1” only. This matrix element possesses the obvious symmetry under the interchange of the nucleon momenta

$$\mathcal{M}_{smm_\gamma m_d}^{(t\mu)}(\mathbf{k}, \mathbf{q}, \mathbf{p}_2, \mathbf{p}_1) = (-)^{s+t+1} \mathcal{M}_{smm_\gamma m_d}^{(t\mu)}(\mathbf{k}, \mathbf{q}, \mathbf{p}_1, \mathbf{p}_2). \quad (17)$$

Choosing the  $z$ -axis in the direction of the incoming photon and isolating the azimuthal dependence of the direction of pion momentum, we obtain the following general form for the reaction matrix

$$\mathcal{M}_{sm, m_\gamma m_d}^{(t\mu)}(\mathbf{k}, \mathbf{q}, \mathbf{p}_1, \mathbf{p}_2) = \mathcal{T}_{sm, m_\gamma m_d}^{(t\mu)}(\mathbf{k}, q, \theta_\pi, \mathbf{p}_1, \mathbf{p}_2) e^{i(m_\gamma + m_d)\phi_\pi}. \quad (18)$$

Using parity conservation one can show, that the reduced  $\mathcal{T}$ -matrix elements obey the following symmetry relation

$$\mathcal{T}_{s, -m, -m_\gamma, -m_d}^{(t\mu)} = (-)^{s+m+m_\gamma+m_d} \mathcal{T}_{s, m, m_\gamma, m_d}^{(t\mu)}. \quad (19)$$

This symmetry relation reduces the number of complex amplitudes from 24 to 12 independent ones. For their determination one needs 23 real observables since a overall phase remains arbitrary.

## 5 Polarization observables

Polarization observables will give additional valuable information for checking the spin degrees of freedom of the elementary pion production amplitude of the neutron, provided, and this is very important, that one has under control all interfering interaction effects which prevent a simple extraction of this amplitude. For the definition of these observables in terms of the transition matrix elements we refer the reader to [44], in which all possible polarization observables in  $d(\gamma, N)N$  with polarized photon beam and/or oriented deuteron target are derived. We briefly recall here the necessary notations and definitions.

The cross section for arbitrary polarized photons and initial deuterons can be computed for a given  $\mathcal{M}$ -matrix by applying the density matrix formalism similar to that given by Arenhövel [44] for deuteron photodisintegration. The most general expression for all possible polarization observables is given by

$$\begin{aligned} \mathcal{O} &= \text{Tr}(\mathcal{M}^\dagger \Omega \mathcal{M} \rho) \\ &= \sum_{\alpha\alpha'} \int d\Omega_{p_{NN}} \rho_s \mathcal{M}_{s'm', m'_\gamma, m'_d}^{(t'\mu')} \star \mathbf{m}_{s'm' sm} \mathcal{M}_{sm, m_\gamma m_d}^{(t\mu)} \\ &\times \rho_{m_\gamma m'_\gamma}^\gamma \rho_{m_d m'_d}^d, \end{aligned} \quad (20)$$

where we have introduced as a shorthand for the quantum numbers  $\alpha' = (s', m', t', m'_\gamma, m'_d)$ .  $\rho_{m_\gamma m'_\gamma}^\gamma$  and  $\rho_{m_d m'_d}^d$  denote the density matrices of initial photon polarization and deuteron orientation, respectively,  $\mathbf{m}_{s'm' sm}$  is an operator associated with the observable, which acts in the two-nucleon spin space and  $\rho_s$  is a phase space factor given in (7). For further details we refer to [44, 45].

As is shown in [44] all polarization observables can be expressed in terms of the quantities

$$\begin{aligned} V_{IM} &= \frac{1}{2\sqrt{3}} \sum_{m'_d m_d} \sum_{sm, m_\gamma} (-)^{1-m'_d} \sqrt{2I+1} \begin{pmatrix} 1 & 1 & I \\ m_d & -m'_d & -M \end{pmatrix} \\ &\times \int d\Omega_{p_{NN}} \rho_s \mathcal{M}_{sm, m_\gamma m_d}^{(t\mu)} \star \mathcal{M}_{sm, m_\gamma m'_d}^{(t\mu)}, \end{aligned} \quad (21)$$

and

$$W_{IM} = \frac{1}{2\sqrt{3}} \sum_{m'_d m_d} \sum_{sm'_d, m_\gamma} (-)^{1-m'_d} \sqrt{2I+1} \begin{pmatrix} 1 & 1 & I \\ m_d & -m'_d & -M \end{pmatrix} \times \int d\Omega_{pNN} \rho_S \mathcal{M}_{sm'_d, m_\gamma, m_d}^{(t\mu)*} \mathcal{M}_{s-m, m_\gamma, -m'_d}^{(t\mu)}, \quad (22)$$

where we use the convention of Edmonds [46] for the Wigner 3j-symbols. These quantities have the symmetry properties

$$\begin{aligned} V_{IM}^* &= (-1)^M V_{I-M}, \\ W_{IM}^* &= (-1)^I W_{IM}. \end{aligned} \quad (23)$$

The unpolarized differential cross section is then given by

$$\frac{d^3\sigma}{d\Omega_\pi dq} = V_{00}. \quad (24)$$

The photon asymmetry for linearly polarized photons is given by

$$\Sigma \frac{d^3\sigma}{d\Omega_\pi dq} = -W_{00}. \quad (25)$$

The vector target asymmetry is given by

$$T_{11} \frac{d^3\sigma}{d\Omega_\pi dq} = 2 \Im m V_{11}. \quad (26)$$

The tensor target asymmetries are given by

$$T_{2M} \frac{d^3\sigma}{d\Omega_\pi dq} = (2 - \delta_{M0}) \Re e V_{2M}, \quad M = 0, 1, 2. \quad (27)$$

The photon and target double polarization asymmetries are given by

(i) Circular

$$T_{1M}^c \frac{d^3\sigma}{d\Omega_\pi dq} = (2 - \delta_{M0}) \Re e V_{1M}, \quad M = 0, 1,$$

$$T_{2M}^c \frac{d^3\sigma}{d\Omega_\pi dq} = 2 \Im m V_{2M}, \quad M = 0, 1, 2, \quad (28)$$

(ii) Longitudinal

$$T_{1M}^\ell \frac{d^3\sigma}{d\Omega_\pi dq} = i W_{1M}, \quad M = 0, \pm 1,$$

$$T_{2M}^\ell \frac{d^3\sigma}{d\Omega_\pi dq} = -W_{2M}, \quad M = 0, \pm 1, \pm 2. \quad (29)$$

Explicit expressions for unpolarized differential cross section and single polarization observables which are predicted and discussed in this work are given in terms of the transition matrix elements in Appendix A.

## 6 Results and discussions

In order to do calculations for pion photoproduction on the deuteron we have to chosen two ingredients for our model: the deuteron wave function and the operator for pion production on a single nucleon.

A large variety of deuteron wave functions is available. They range from simple Hulthén or Yamaguchi-type wave functions to wave functions obtained from modern  $NN$  potentials. The contribution to the pion production amplitude

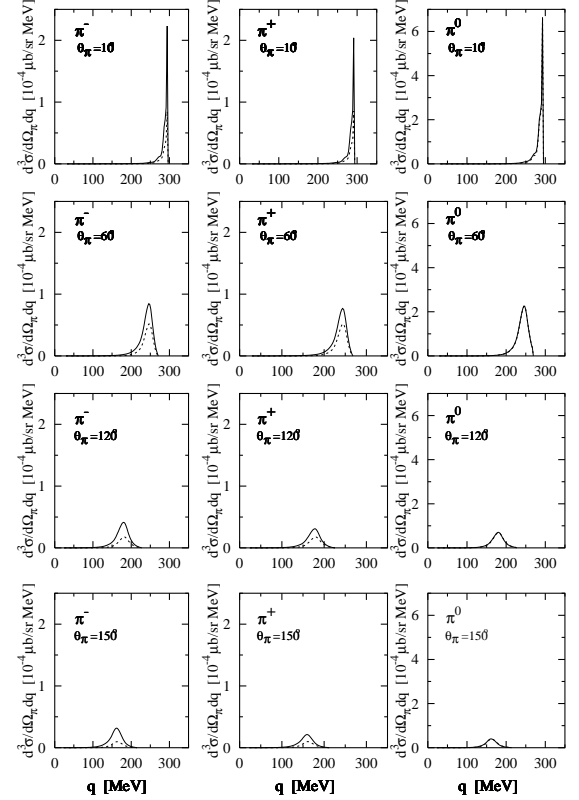


**Fig. 6:** The  $\pi$ -meson spectra in the  $d(\gamma, \pi)NN$  reaction as a function of the absolute value of pion momentum  $q$  at a photon energy of 330 MeV for four different values of emission pion angles  $\theta_\pi$ . The solid curves show the results of the full calculations while the dotted curves represent the results when only the  $\Delta(1232)$ -resonance is taken into account. The left, middle and right panels represent the results for  $\gamma d \rightarrow \pi^- pp$ ,  $\pi^+ nm$  and  $\pi^0 np$ , respectively.

in (16) is evaluated by taking a realistic  $NN$  potential model for the deuteron wave function. For our calculations we have used the wave function of the Paris potential [47], which is in excellent agreement with  $NN$  scattering data [48].

The most important ingredient of the model is the operator for pion photoproduction on a single nucleon. This operator is obtained in this work by computing the nonrelativistic reduction of the amplitudes for the Feynman diagrams in Fig. 1. As already seen in section 2, that our calculations for the elementary process are in good agreement with recent experimental data as well as with other theoretical predictions and gave a clear indication that this elementary operator is quite satisfactory for our purpose.

The discussion of our results is divided into four parts. First, we will discuss the  $\pi$ -meson spectra as a function of the absolute value of pion momentum  $q$  at forward and backward emission pion angles  $\theta_\pi$  for photon energy at the  $\Delta(1232)$ -resonance region, i.e.  $\omega_\gamma^{\text{lab}} = 330$  MeV. In the second part, we will then consider the photon asymmetry  $\Sigma$  for linearly polarized photons. Our results for the vector target asymmetry  $T_{11}$  will be presented in the third part. In the last part, we will discuss our results for the tensor target asymmetries  $T_{20}$ ,  $T_{21}$ ,

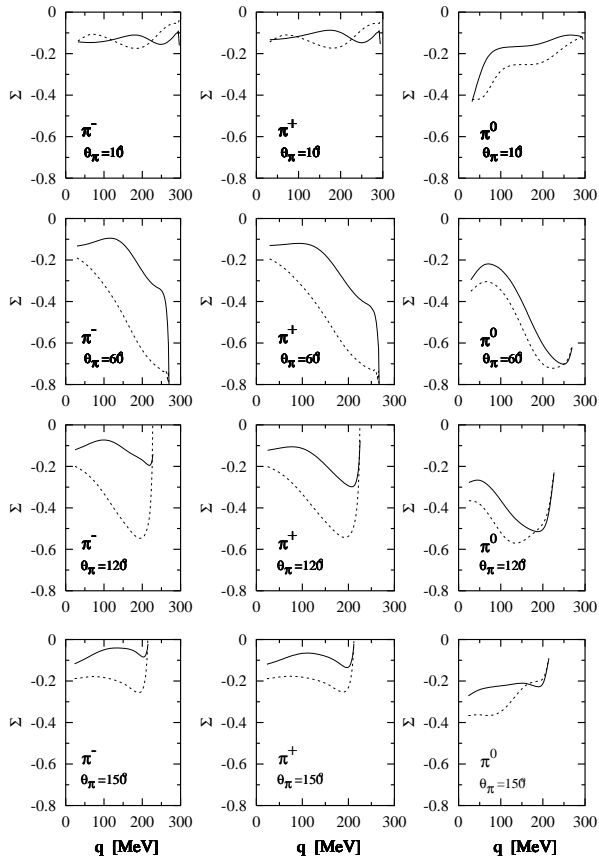


**Fig. 7:** Photon asymmetry  $\Sigma$  of  $d(\gamma,\pi)NN$ . Notation of the curves as in Fig. 6.

and  $T_{22}$ . In all parts, we will give a calculations for all the three isospin channels of the  $d(\gamma,\pi)NN$  reaction. For comparison, we will always present the results for the full calculation and the results when only the  $\Delta(1232)$ -resonance contribution is taken into account.

All the above mentioned observables are calculated, as seen in Appendix A, by integrating over the polar angle  $\theta_{p_{NN}}$  and the azimuthal angle  $\phi_{p_{NN}}$  of the relative momentum  $\mathbf{p}_{NN}$  of the two outgoing nucleons. These integrations are carried out numerically. The number of integration points was being increased until the accuracy of calculated observable becomes good to 1%.

### 6.1 The $\pi$ -meson spectra

We start our discussion with the  $\pi$ -meson spectra, i.e., the unpolarized differential cross section  $d^3\sigma/(d\Omega_\pi dq)$  which comes from the fully exclusive differential cross section  $d^5\sigma/(d\Omega_\pi dq d\Omega_{p_{NN}})$  by integrating over  $\Omega_{p_{NN}}$ . In Fig. 6 we depict our results for the  $\pi$ -meson spectra as a function of the absolute value of pion momentum  $q$  at four different values of emission pion angles  $\theta_\pi$  for each isospin channel of the  $\gamma d \rightarrow \pi NN$  reaction for  $\omega_\gamma^{lab} = 330$  MeV. One sees, that when the absolute value of pion momentum  $q$  reaches its maximum,

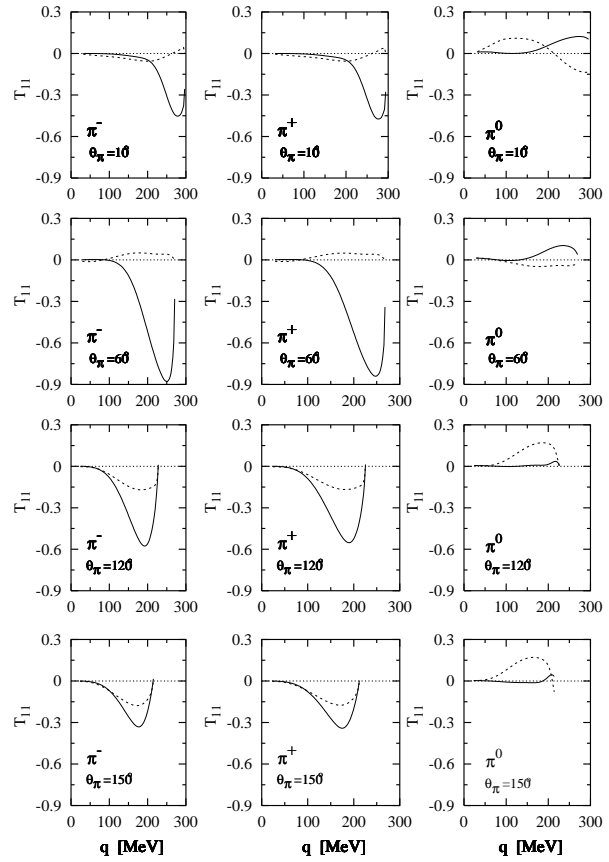


**Fig. 8:** Vector target asymmetry  $T_{11}$  of  $d(\gamma,\pi)NN$ . Notation of the curves as in Fig. 6.

the absolute value of the relative momentum  $p_{NN}$  of the two outgoing nucleons vanishes, and thus a narrow peak appears in the forward emission pion angles for charged as well as for neutral pion photoproduction channels. In the lower part of Fig. 6 we see, that the unpolarized differential cross section is small and the narrow peak which appears at forward emission pion angles disappears. The same effect appears in the coherent process of charged pion photo- and electroproduction on the deuteron [49,50], in deuteron electrodisintegration [51] as well as in  $\eta$ -photoproduction [52]. It is also clear that the maximum value of  $q$  (when  $p_{NN} \rightarrow 0$ ) decreases with increasing the emission pion angle. It changes from  $\sim 300$  MeV at forward emission angles to  $\sim 200$  MeV at backward ones. In principle, the experimental observation of this peak in the high  $\pi$ -momentum spectrum may serve as another evidence for the understanding of the  $\pi$ -meson spectra.

In conclusion, one notes that the contributions from Born terms are important for charged pion production channels but these are much less important in the case of neutral pion production.

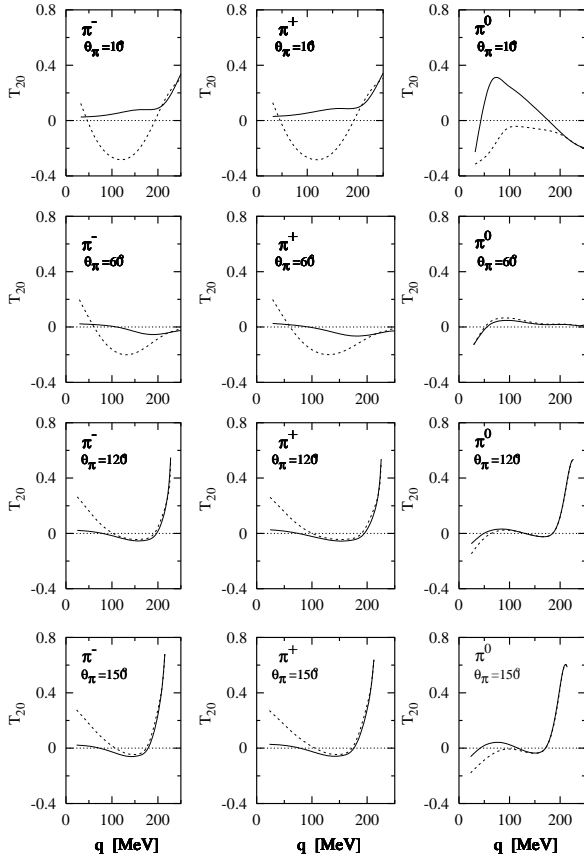


**Fig. 9:** Tensor target asymmetry  $T_{20}$  of  $d(\gamma, \pi)NN$ . Notation of the curves as in Fig. 6.

## 6.2 Photon asymmetry

Here we discuss our results for the photon asymmetry  $\Sigma$  for linearly polarized photons for all the different charge states of the pion of  $d(\gamma, \pi)NN$ . The  $\gamma$ -asymmetry for fixed pion angles of  $10^\circ$ ,  $60^\circ$ ,  $120^\circ$ , and  $150^\circ$  are plotted in Fig. 7 as a function of the absolute value of pion momentum  $q$  at  $\omega_\gamma^{lab} = 330$  MeV. The dotted curves show the contribution of the  $\Delta(1232)$ -resonance alone in order to clarify the importance of the Born terms. First of all, we see that the photon asymmetry has always a negative values at forward and backward emission pion angles for charged as well as for neutral pion channels. One notes qualitatively a similar behaviour for charged pion channels whereas a totally different behaviour is seen for the neutral pion channel.

For extreme forward and backward pion angles one sees, that the effect of Born contributions is relatively small in comparison to the results at  $\theta_\pi = 60^\circ$  and  $120^\circ$ . At  $60^\circ$  we see a strong reduction of the photon asymmetry at maximum pion momentum. This reduction changes to an overestimation at backward pion angles. One notices also, that the contributions from Born terms are much important, in particular at  $q \simeq 200$  MeV which is very clear for charged pion channels. We observe that the interference of the Born terms with the  $\Delta(1232)$ -resonance contribution causes considerable changes in

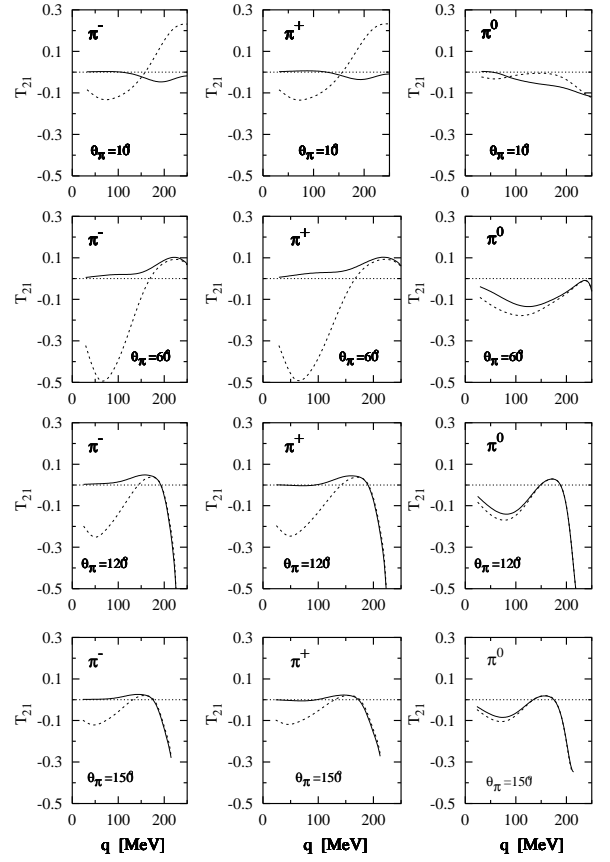


**Fig. 10:** Tensor target asymmetry  $T_{21}$  of  $d(\gamma, \pi)NN$ . Notation of the curves as in Fig. 6.

the photon asymmetry. Experimental measurements as well as other theoretical predictions will give us more valuable information on the photon asymmetry.

## 6.3 Vector target asymmetry

In this subsection we present and discuss our results for the vector target asymmetry  $T_{11}$ . Fig. 8 shows these results as a function of the absolute value of pion momentum  $q$  at four different values of pion angles  $\theta_\pi$  for  $\omega_\gamma^{lab} = 330$  MeV. The asymmetry  $T_{11}$  clearly differs in size between charged and neutral pion photoproduction channels, being even opposite in phase. For charged pion photoproduction reactions we see from the left and middle panels of Fig. 8, that the vector target asymmetry has always a negative values. At forward pion angles these values come mainly from the Born terms since a small contribution from the  $\Delta$ -resonance was found. At backward angles, the negative values come from an interference of the Born terms with the  $\Delta(1232)$ -resonance contribution since the  $\Delta$ -contribution is large in this case.

With respect to the neutral pion photoproduction reaction, we see from the solid curves of the right panel of Fig. 8, that the vector target asymmetry  $T_{11}$  has a very small negative values at smaller pion momentum and a relatively large positive values at

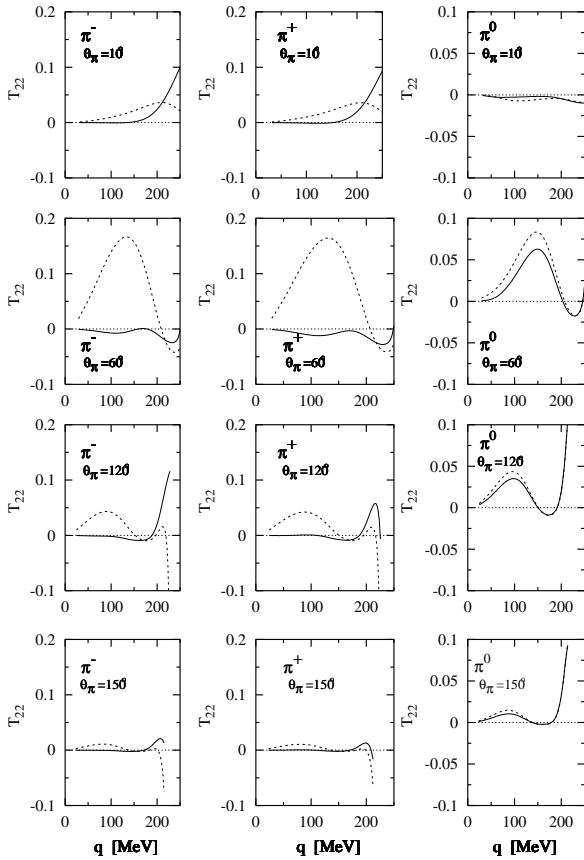


**Fig. 11:** Tensor target asymmetry  $T_{22}$  of  $\mathbf{d}(\gamma, \pi)NN$ . Notation of the curves as in Fig. 6.

higher pion momentum. It is interesting to point out the importance of the Born terms in the charged pion production reactions in comparison to the contribution of the  $\Delta(1232)$ -resonance. The sensitivity of  $T_{11}$  to the Born terms has also been discussed by Blaazer *et al.* [53] and Wilhelm and Arenhövel [54] for the coherent pion photoproduction reaction on the deuteron. The reason is that  $T_{11}$  depends on the relative phase of the matrix elements as can be seen from (21) and (26). It would vanish for a constant overall phase of the  $t$ -matrix, a case which is approximately realized if only the  $\Delta(1232)$ -amplitude is considered.

#### 6.4 Tensor target asymmetries

Let us present and discuss now the results of the tensor target asymmetries  $T_{20}$ ,  $T_{21}$ , and  $T_{22}$  for  $\mathbf{d}(\gamma, \pi)NN$ . We start from the tensor asymmetry  $T_{20}$ . For  $\gamma d \rightarrow \pi NN$  at forward and backward emission pion angles, the asymmetry  $T_{20}$  allows one to draw specific conclusions about details of the reaction mechanism. Results for  $T_{20}$  are plotted in Fig. 9 at four different values of pion angles as a function of the absolute value of pion momentum  $q$  for  $\omega_{\gamma}^{\text{lab}} = 330$  MeV. The dotted curves represent our results for the contribution of the  $\Delta(1232)$ -resonance and the solid ones show the results when the Born terms are included. In

general, one notes again the importance of Born terms in the case of charged pion photoproduction channels (see the left and middle panels of Fig. 9). In the case of neutral pion production channel (right panel of Fig. 9) one sees, that the Born terms are important only at extreme forward pion angles. One sees also that the contribution of Born terms is very small for backward pion angles and higher pion momentum, but it is relatively large for small pion momentum.

Fig. 10 shows our results for the tensor target asymmetry  $T_{21}$  as a function of  $q$  for fixed pion angles  $\theta_{\pi} = 10^{\circ}$ ,  $60^{\circ}$ ,  $120^{\circ}$ , and  $150^{\circ}$  at  $\omega_{\gamma}^{\text{lab}} = 330$  MeV. The dotted curves are due to calculations done without the inclusion of the Born terms. One notices that the  $T_{21}$  asymmetry is sensitive to Born terms, in particular at forward pion angles. Also in this case one notes the importance of Born terms in the case of charged pion photoproduction reactions, in particular at smaller pion momentum. In the case of  $\pi^0$  channel one sees that the contribution of Born terms is much less important at all angles.

In Fig. 11 we depict our results for the tensor target asymmetry  $T_{22}$  as a function of  $q$ . We have used here the same four values of pion angle  $\theta_{\pi}$  as in the previous figures. One readily notes the importance of Born terms, in particular for charged pion channels. Like the results of Figs. 9 and 10, the  $T_{22}$  asymmetry is sensitive to the values of pion angle  $\theta_{\pi}$ . We notice that the  $T_{22}$  asymmetry changes dramatically if only the  $\Delta$ -contribution is taken into account. At  $\theta_{\pi} = 60^{\circ}$  we see that the Born terms are very important, especially for charged pion photoproduction channels. In the case of neutral pion production channel these terms are much less important.

## 7 Conclusions

In this paper we have studied incoherent single pion photoproduction on the deuteron in the  $\Delta(1232)$ -resonance region with special emphasis on polarization observables. The  $\gamma d \rightarrow \pi NN$  scattering amplitude is given as a linear combination of the on-shell matrix elements of pion photoproduction on the two nucleons. For the elementary pion photoproduction operator an effective Lagrangian model is used which is based on time-ordered perturbation theory and describes well the elementary  $\gamma N \rightarrow \pi N$  reaction.

Particular attention was paid to  $\pi$ -meson spectra as well as single polarization observables. We have presented results for the unpolarized differential cross section  $d^3\sigma/d\Omega_{\pi}dq$ , photon asymmetry  $\Sigma$  for linearly polarized photons, vector target asymmetry  $T_{11}$  and tensor target asymmetries  $T_{20}$ ,  $T_{21}$ , and  $T_{22}$ . As already noticed in the discussion above, we found that interference of Born terms and the  $\Delta(1232)$ -contribution plays a significant role. Unfortunately, there are no experimental data available to be compared to the observables we computed.

We would like to conclude that the results presented here for polarization observables in the  $d(\gamma, \pi)NN$  reaction in the  $\Delta$ -resonance region can be used as a basis for the simulation of the behaviour of polarization observables and for an optimal planning of new polarization experiments of this reaction. It would be very interesting to examine our predictions experimentally.

Finally, we would like to point out that future improvements of the present model should include further investigations

including a three-body treatment of the final  $\pi NN$  system for the lowest and most important partial waves. As future refinements we consider also the use of a more sophisticated elementary production operator, which will allow one to extend the present approach to higher energies, and the role of irreducible two-body contributions to the electromagnetic pion production operator.

## A Explicit expressions for polarization observables

In this appendix we give the formal expressions for unpolarized differential cross section and single polarization observables which are presented and discussed in this paper. The 3-fold unpolarized differential cross section is obtained from the fully exclusive differential cross section (6) by integration over  $\Omega_{PNN}$

$$\frac{d^3\sigma}{d\Omega_\pi dq} = \frac{1}{6} \mathcal{F} \quad (30)$$

with

$$\mathcal{F} = \sum_\alpha \int d\Omega_{PNN} \rho_S |\mathcal{M}_{smm_\gamma, m_d}^{(t\mu)}|^2. \quad (31)$$

The photon asymmetry for linearly polarized photons is given by

$$\begin{aligned} \Sigma &= \frac{d\sigma^\parallel - d\sigma^\perp}{d\sigma^\parallel + d\sigma^\perp} \\ &= \frac{2}{\mathcal{F}} \Re e \sum_{s,m,t,m_d} \int d\Omega_{PNN} \rho_S \mathcal{M}_{sm+1m_d}^{(t\mu)} \mathcal{M}_{sm-1m_d}^{(t\mu)*}, \end{aligned} \quad (32)$$

where  $d\sigma^{\parallel(\perp)}$  is the differential cross section for incoming photons polarized parallel (perpendicular) to the reaction plane.

The vector target asymmetry  $T_{11}$  is given by

$$\begin{aligned} T_{11} &= \frac{\sqrt{6}}{\mathcal{F}} \Im m \sum_{s,m,t,m_\gamma} \int d\Omega_{PNN} \rho_S \left[ \mathcal{M}_{smm_\gamma-1}^{(t\mu)} - \mathcal{M}_{smm_\gamma+1}^{(t\mu)} \right] \\ &\quad \times \mathcal{M}_{smm_\gamma,0}^{(t\mu)*}. \end{aligned} \quad (33)$$

The tensor target asymmetries are expressed in terms of the amplitudes as follows

$$\begin{aligned} T_{20} &= \frac{1}{\sqrt{2}\mathcal{F}} \sum_{s,m,t,m_\gamma} \int d\Omega_{PNN} \rho_S \left[ |\mathcal{M}_{smm_\gamma+1}^{(t\mu)}|^2 + |\mathcal{M}_{smm_\gamma-1}^{(t\mu)}|^2 \right. \\ &\quad \left. - 2 |\mathcal{M}_{smm_\gamma,0}^{(t\mu)}|^2 \right], \end{aligned} \quad (34)$$

$$\begin{aligned} T_{21} &= \frac{\sqrt{6}}{\mathcal{F}} \Re e \sum_{s,m,t,m_\gamma} \int d\Omega_{PNN} \rho_S \left[ \mathcal{M}_{smm_\gamma-1}^{(t\mu)} - \mathcal{M}_{smm_\gamma+1}^{(t\mu)} \right] \\ &\quad \times \mathcal{M}_{smm_\gamma,0}^{(t\mu)*}, \end{aligned} \quad (35)$$

$$T_{22} = \frac{2\sqrt{3}}{\mathcal{F}} \Re e \sum_{s,m,t,m_\gamma} \int d\Omega_{PNN} \rho_S \mathcal{M}_{smm_\gamma-1}^{(t\mu)} \mathcal{M}_{smm_\gamma+1}^{(t\mu)*}. \quad (36)$$

## References

- [1] B. Krusche and S. Schadmand, *Prog. Part. Nucl. Phys.* **51** (2003) 399; V. Burkert and T.-S.H. Lee, *Int. J. Mod. Phys. E* **13** (2004) 1035; B. Krusche, *Prog. Part. Nucl. Phys.* **55** (2005) 46; H. Dutz *et al.*, *Phys. Rev. Lett.* **94** (2005) 162001; K. Helbing, *Prog. Part. Nucl. Phys.* **57** (2006) 405; J. Ahrens *et al.*, *Phys. Rev. Lett.* **97** (2006) 202303; B. Krusche and I. Jägle, *Acta Phys. Pol. B Proc. Suppl.* **2** (2009) 51; J. Ahrens *et al.*, *Phys. Lett. B* **672** (2009) 328; Y. Ilieva *et al.* [CLAS Collaboration], *Eur. Phys. J. A* **43** (2010) 261; J. Ahrens *et al.*, *Eur. Phys. J. A* **44** (2010) 189; I. A. Rachek *et al.*, *J. Phys. Conf. Ser.* **295** (2011) 012106; B. Krusche, *Eur. Phys. J. Spec. Top.* **198** (2011) 199; D. K. Hasell *et al.*, *Ann. Rev. Nucl. Part. Sci.* **61** (2011) 409; B. Strandberg *et al.*, *EPJ Web Conf.* **130** (2016) 05019; D. M. Nikolenko *et al.*, *Phys. Part. Nucl.* **48** (2017) 102; F. Cividini [A2@MAMI Collaboration], *EPJ Web Conf.* **199** (2019) 02007; S. E. Lukonin *et al.*, *Int. J. Mod. Phys. E* **28** (2019) 1950010; B. Strandberg *et al.*, *Phys. Rev. C* **101** (2020) 035207; B. Krusche, *Acta Phys. Pol. B* **51** (2020) 61.
- [2] See, or example, the IUPAP Report 41: A Worldwide Perspective Of Research And Research Facilities in Nuclear Physics by the IUPAP Working Group 9, <http://www.iupap.org/wg/>.
- [3] E. M. Darwish, H. Arenhövel, and M. Schwamb, *Eur. Phys. J. A* **16** (2003) 111.
- [4] E. M. Darwish, H. Arenhövel, and M. Schwamb, *Eur. Phys. J. A* **17** (2003) 513.
- [5] I. T. Obukhovskiy *et al.*, *J. Phys. G* **29** (2003) 2207.
- [6] H. Arenhövel, A. Fix, and M. Schwamb, *Phys. Rev. Lett.* **93** (2004) 202301.
- [7] A. Fix and H. Arenhövel, *Phys. Rev. C* **72** (2005) 064005.
- [8] V. Lensky, V. Baru, J. Haidenbauer, C. Hanhart, A. Kudryavtsev, and U.-G. Meißner, *Eur. Phys. J. A* **26** (2005) 107.
- [9] M. I. Levchuk *et al.*, *Phys. Rev. C* **74** (2006) 014004.
- [10] E. M. Darwish, C. Fernández-Ramírez, E. Moya de Guerra, and J. M. Udías, *Phys. Rev. C* **76** (2007) 044005.
- [11] E. M. Darwish, M. A. Shehata, and S. S. Al-Thoyaib, *Chin. J. Phys.* **45** (2007) 432.
- [12] M. I. Levchuk, *Phys. Rev. C* **82** (2010) 044002.
- [13] V. E. Tarasov *et al.*, *Phys. Rev. C* **84** (2011) 035203; V. E. Tarasov *et al.*, *Phys. Atom. Nucl.* **79** (2016) 216.
- [14] E. M. Darwish and S. S. Al-Thoyaib, *Ann. Phys. (N.Y.)* **326** (2011) 604.
- [15] E. M. Darwish, *Appl. Math. & Inf. Sci.* **9** (2015) 527 and references therein.
- [16] E. M. Darwish, H. M. Abou-Elsebaa, E. A. Sultan, and Kh. S. A. Hassaneen, *Int. J. Mod. Phys. E* **26** (2017) 1750059.
- [17] S. X. Nakamura, *Phys. Rev. C* **98** (2018) 042201; S. X. Nakamura, H. Kamano, and T. Sato, *Phys. Rev. D* **99** (2019) 031301; S. X. Nakamura, H. Kamano, T.-S. H. Lee, and T. Sato, arXiv:nucl-th/1804.04757.
- [18] A. Fix and H. Arenhövel, *Phys. Rev. C* **100** (2019) 034003.
- [19] E. M. Darwish *et al.*, *Ann. Phys. (N.Y.)* **411** (2019) 167990.
- [20] E. M. Darwish, M. M. Almarashi, and M. Saleh Yousef, *Ann. Phys. (N.Y.)* **420** (2020) 168254; E. M. Darwish and H. M. Al-Ghamdi, *Int. J. Mod. Phys. E*, (2020), DOI: <https://doi.org/10.1142/S0218301320500561>.

- [21] E. S. Kokoulina, M. I. Levchuk, M. N. Nevmerzhitsky, and R. G. Shulyakovsky, Doklady of the National Academy of Sciences of Belarus **64** (2020) 159 (in Russian).
- [22] E. M. Darwish, M. Levchuk, M. N. Nevmerzhitsky, M. M. Almarashi, and M. Saleh Yousef, Chin. J. Phys. **71**, 319 (2021).
- [23] R.G. Arnold, C.E. Carlson, and F. Gross, Phys. Rev. C **23**, 363 (1981).
- [24] H. Arenhövel, W. Leidemann, and E.L. Tomusiak, Z. Phys. A **331**, 509 (1988).
- [25] F. Klein *et al.*, in Proceedings of the 14th International Conference on Particle and Nuclei, Williamsburg, 1996, ed. C.E. Carlson and J.J. Domingo (World Scientific, Singapore, 1996) p. 21.
- [26] E.M. Darwish, H. Arenhövel, and M. Schwamb, Eur. Phys. J. A **16**, 111 (2003).
- [27] E.M. Darwish, H. Arenhövel, and M. Schwamb, Eur. Phys. J. A **17**, 513 (2003).
- [28] R. Schmidt, H. Arenhövel, and P. Wilhelm, Z. Phys. A **355**, 421 (1996); R. Schmidt, Diploma thesis, Institut für Kernphysik, Johannes Gutenberg-Universität, Mainz, Germany, 1995.
- [29] E. Breitmoser and H. Arenhövel, Nucl. Phys. A **612**, 321 (1997); E. Breitmoser, Diploma thesis, Institut für Kernphysik, Johannes Gutenberg-Universität, Mainz, Germany, 1995.
- [30] D. Drechsel, O. Hanstein, S.S. Kamalov, and L. Tiator, MAID: [www.kph.uni-mainz.de/de/MAID/maid2000/](http://www.kph.uni-mainz.de/de/MAID/maid2000/), Institut für Kernphysik, Johannes Gutenberg-Universität, Mainz, Germany.
- [31] O. Hanstein, D. Drechsel, and L. Tiator, Nucl. Phys. A **632**, 561 (1998).
- [32] R.A. Arndt *et al.*, SAID via telnet VTINTE.PHYS.VT.EDU, Virginia Polytechnic Institute, Blacksburg, Virginia.
- [33] R. Beck *et al.*, Phys. Rev. Lett. **78**, 606 (1997); R. Beck *et al.*, Phys. Rev. C **61**, 035204 (2000); H.-P. Krahn, PhD thesis, Johannes Gutenberg-Universität, Mainz, Germany, 1996.
- [34] R. Leukel, PhD thesis, Johannes Gutenberg-Universität, Mainz, Germany, 2001.
- [35] I. Preobrajenski, PhD thesis, Johannes Gutenberg-Universität, Mainz, Germany, 2001.
- [36] T. Fujii *et al.*, Nucl. Phys. B **120**, 395 (1977).
- [37] A. Bagheri *et al.*, Phys. Rev. C **38**, 875 (1988).
- [38] F. Härter, PhD thesis, Institut für Kernphysik, Johannes Gutenberg-Universität, Mainz, Germany, 1996.
- [39] J.D. Bjorken and S.D. Drell, *Relativistic Quantum Mechanics* (McGraw-Hill, New York, 1964).
- [40] P. Osland and A.K. Rej, Nuovo Cimento A **32**, 469 (1976).
- [41] C. Lazard, R.J. Lombard, and Z. Maric, Nucl. Phys. A **271**, 317 (1976).
- [42] P. Bosted and J.M. Laget, Nucl. Phys. A **296**, 413 (1978).
- [43] M.P. Rekalov and I.V. Stoletnii, J. Phys. G **17**, 1643 (1991).
- [44] H. Arenhövel, Few-Body Syst. **4**, 55 (1988).
- [45] B.A. Robson, *The Theory of Polarization Phenomena* (Clarendon Press, Oxford, 1974).
- [46] A.R. Edmonds, *Angular Momentum in Quantum Mechanics* (Princeton University Press, New Jersey, 1957).
- [47] M. Lacombe *et al.*, Phys. Lett. B **101**, 139 (1981).
- [48] E.M. Darwish, PhD thesis, Institut für Kernphysik, Johannes Gutenberg-Universität, Mainz, Germany, 2002, nucl-th/0303056.
- [49] J.-M. Laget, Nucl. Phys. A **296**, 388 (1978).
- [50] G. Köbschall *et al.*, Nucl. Phys. A **466**, 612 (1987).
- [51] W. Fabian and H. Arenhövel, Nucl. Phys. A **258**, 461 (1976).
- [52] A. Fix and H. Arenhövel, Z. Phys. A **359**, 427 (1997).
- [53] F. Blaaizer, B.L.G. Bakker, and H.J. Boersma, Nucl. Phys. A **568**, 681 (1994).
- [54] P. Wilhelm and H. Arenhövel, Nucl. Phys. A **593**, 435 (1995).